Seminal vesicle protein SVS2 is required for sperm survival in the uterus

Natsuko Kawano[a], Naoya Araki[b], Kaoru Yoshida[c], Taku Hibino[d], Naoko Ohnami[a], Maako Makino[a], Seiya Kanai[a], Hidetoshi Hasuwa[e], Manabu Yoshida[b,1], Kenji Miyado[a,1], and Akihiro Umezawa[a]

[a]Department of Reproductive Biology, National Center for Child Health and Development, 2-10-1 Okura, Setagaya, Tokyo 157-8535, Japan; [b]Misaki Marine Biological Station, Graduate School of Science, University of Tokyo, Miura, Kanagawa 238-0225, Japan; [c]Biomedical Engineering Center, Toin University of Yokohama, Yokohama 225-8502, Japan; [d]Faculty of Education, Saitama University, 255 Shimo-Okubo, Sakura-ku, Saitama City, Saitama 338-8570, Japan; and [e]Research Institute for Microbial Diseases, Osaka University, Yamadaoka 3-1, Suita, Osaka 565-0871, Japan

Edited by John J. Eppig, The Jackson Laboratory, Bar Harbor, ME, and approved February 11, 2014 (received for review November 12, 2013)

In mammals, sperm migrate through the female reproductive tract to reach the egg; however, our understanding of this journey is highly limited. To shed light on this process, we focused on defining the functions of seminal vesicle secretion 2 (SVS2). *SVS2*$^{-/-}$ male mice produced sperm but were severely subfertile, and formation of a copulatory plug to cover the female genital opening did not occur. Surprisingly, even when artificial insemination was performed with silicon as a substitute for the plug, sperm fertility in the absence of SVS2 remained severely reduced because the sperm were already dead in the uterus. Thus, our results provide evidence that the uterus induces sperm cell death and that SVS2 protects sperm from uterine attack.

in vivo fertilization | uterine sperm selection | decapacitation | acrosomal reaction | uterine spermicide

Fluids secreted from male accessory sex organs are believed to regulate fertility efficiency through the control of sperm functions such as motility and fertilizing ability in vivo (1, 2). Notably, the induced ability of fertilization-competent (i.e., capacitated) rabbit sperm is reverted to an incompetent state when it is mixed with seminal plasma; this phenomenon, discovered by Chang and Bedford (2, 3), is referred to as "decapacitation." Subsequent to their findings, many studies have focused on identifying the decapacitation factor in the seminal plasma using in vitro assays (4–6); the seminal plasma is believed to stabilize sperm plasma membranes and prevent uterine sperm from undergoing premature capacitation and acrosomal reaction, an exocytotic process that occurs immediately before sperm–egg fusion (7, 8).

In mammals the seminal vesicle is an accessory organ within the male reproductive tract, and its secretion influences sperm fertility and embryo development via oviductal expression of cytokines (9). Seminal vesicle secretion 2 (SVS2), a major component of the seminal vesicle secretions, inhibits sperm fertility in vitro, and homologous genes are conserved among many species (10, 11). As described previously (10), SVS2 binds to sperm in the uterus but not to sperm in the oviduct. In addition, SVS2 binds to ganglioside GM1 as its receptor on the sperm membrane, resulting in the control of sperm fertility (11). To study the role of SVS2 in vivo, we here focused on defining a role for SVS2 in in vivo fertilization.

Results

To explore the physiological role of SVS2, we produced mice lacking the *SVS2* gene (*SI Appendix*, Fig. S1). Two independent ES cell lines carrying a mutated allele were used to generate chimeric mice capable of transmitting the mutated allele to their progeny. Homozygous (*SVS2*$^{-/-}$) mice were identified by Southern blot and PCR analyses of genomic DNA. The same results were obtained for both mouse lines used. Breeding yielded the predicted number of null mice at Mendelian frequency. Both male and female *SVS2*$^{-/-}$ mice were born healthy, grew normally, and had normally configured seminal vesicles (Fig. 1*A* and *SI Appendix*, Fig. S2*A*). The loss of SVS2 in the *SVS2*$^{-/-}$ mice was confirmed by SDS/PAGE using total proteins collected from seminal vesicles (Fig. 1*B* and *SI Appendix*, Fig. S3*B*). Moreover, electron microscopic analysis of the seminal vesicle epithelium revealed the presence of normal features, such as secretory organelles, in *SVS2*$^{-/-}$ mice as well as in *SVS2*$^{+/+}$ mice (*SI Appendix*, Fig. S2*B*).

Despite the absence of detrimental effects on seminal vesicle formation, *SVS2*$^{-/-}$ male mice displayed strongly reduced fertility: the average litter size produced by the *SVS2*$^{-/-}$ male mice was significantly smaller (0.63 ± 0.13) than those of the *SVS2*$^{+/+}$ and *SVS2*$^{+/-}$ male mice (5.23 ± 0.53 and 4.96 ± 0.42, respectively; $P < 0.001$) (Fig. 1*C*). Copulatory plugs were not found in female mice mated with *SVS2*$^{-/-}$ male mice (Fig. 1*A*), although mating behavior was observed and sperm were normally produced in these mice (*SI Appendix*, Fig. S4*A*). In addition, the rates of motile and hyperactivated sperm, evaluated by computer assisted sperm analysis (CASA), were indistinguishable between *SVS2*$^{-/-}$ and *SVS2*$^{+/+}$ male mice (*SI Appendix*, Fig. S4 *B* and *C*). When the epididymal sperm of *SVS2*$^{-/-}$ male mice were subjected to in vitro fertilization (IVF), the rate of fertilized eggs (based on the evaluation of pronuclear formation) was comparable to those of sperm from *SVS2*$^{+/+}$ and *SVS2*$^{+/-}$ male mice (*SI Appendix*, Fig. S4*D*). From these results, we concluded that SVS2 might be essential for plug formation but not spermatogenesis or in vitro sperm fertility.

Significance

Male mice lacking seminal vesicle secretion 2 (SVS2) protein, which is a major component of seminal vesicle secretions, display prominently reduced fertility. However, their epididymal sperm are able to fertilize eggs normally in vitro, suggesting that SVS2 is only essential for in vivo fertilization. We demonstrate that infertility in *SVS2*$^{-/-}$ male mice is caused not only by failed copulatory plug formation but also by the disruption of ejaculated sperm in the uterus by uterus-derived cytotoxic factors. SVS2 acts to protect sperm against these uterus-derived cytotoxic factors by coating the sperm surface and preventing uterine attack. Thus, our results provide evidence that mammalian males have developed a protective strategy against female attack at the gamete level.

Author contributions: N.K., K.Y., M.Y., and K.M. designed research; N.K., N.A., T.H., N.O., M.M., S.K., H.H., and K.M. performed research; N.K., M.Y., K.M., and A.U. analyzed data; and N.K. and K.M. wrote the paper.

The authors declare no conflict of interest.

This article is a PNAS Direct Submission.

Freely available online through the PNAS open access option.

[1]To whom correspondence may be addressed. E-mail: yoshida@mmbs.s.u-tokyo.ac.jp or miyado-k@ncchd.go.jp.

This article contains supporting information online at www.pnas.org/lookup/suppl/doi:10.1073/pnas.1320715111/-/DCSupplemental.

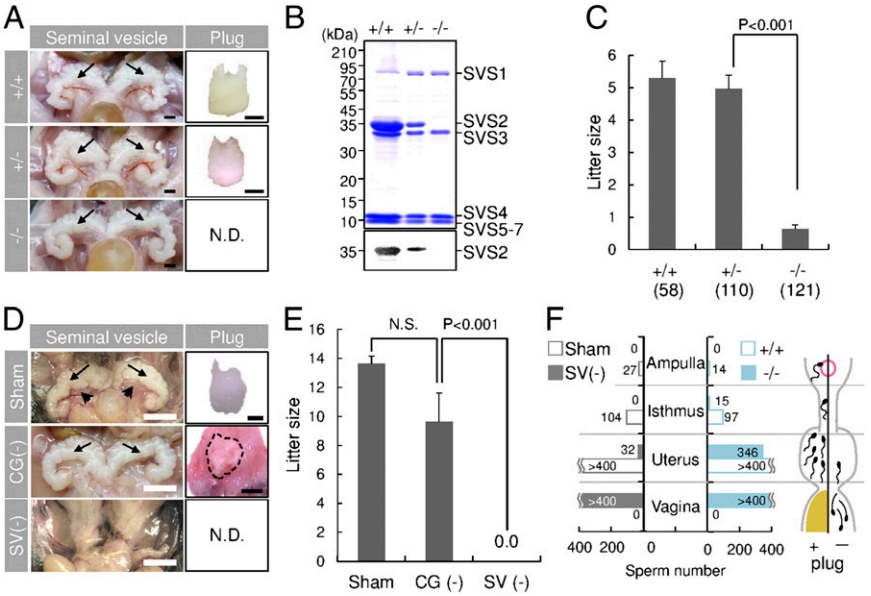

Fig. 1. Impaired copulatory plug formation in *SVS2*$^{-/-}$ and seminal vesicle-excised mice. (*A*) Appearance of seminal vesicles and copulatory plugs. Arrows, seminal vesicles. N.D., not detected. (Scale bars, 2 mm.) (*B*) Immunoblotting of the total inner fluid of seminal vesicles isolated from male mice with anti-SVS2 pAb. (*Upper*) Staining with CBB; (*Lower*) reaction with anti-SVS2 pAb. (*C*) Fecundity of male mice. Parentheses, numbers of male mice examined. (*D*) Appearance of seminal vesicles and copulatory plugs in surgically operated mice. Sham, sham-operated mice; CG(-), mice with coagulating glands excised; SV(-), mice with seminal vesicles excised. Arrows, seminal vesicles; arrowheads, coagulating glands; dotted circle, a representative plug formed by a CG(-) male mouse. (Scale bars, 2 mm.) (*E*) Fecundity of surgically operated male mice ($n = 5$). N.S., not significant. (*F*) Numbers of sperm entering the female reproductive tract after copulation. The total sperm number is indicated as the sum of five independent experiments. (*Right graph*) Number of sperm detected in each sectioned tract of female mice mated with *SVS2*$^{+/+}$ or *SVS2*$^{-/-}$ male mice. (*Left graph*) Number of sperm detected in each sectioned tract of female mice mated with Sham or SV(-) male mice.

The phenotypes of gene-deficient mice are not always related to the disrupted gene itself but are sometimes caused by the disruption of a neighboring gene (12). To examine whether the phenotype observed for *SVS2*$^{-/-}$ mice was directly derived from the lack of SVS2, two transgenic mouse lines expressing SVS2 in the seminal vesicles were generated and introduced into the *SVS2*$^{-/-}$ background. We found that introduction of the transgene recovered plug formation (*SI Appendix*, Fig. S5*A*) and the reduced fecundity in *SVS2*$^{-/-}$ male mice (*SI Appendix*, Fig. S5*B*). These results suggest that SVS2 plays a role in plug formation and imply that loss of plug formation may lead to male infertility.

When the male accessory sex glands, coagulating glands (arrowheads in Fig. 1*D*) or seminal vesicles (arrows in Fig. 1*D*), were surgically removed, the average litter size produced by the mice after coagulating gland removal was 9.6 ± 2.0, which was comparable to that of the control mice (13.6 ± 0.5) (Fig. 1*E*). In contrast, mice that had undergone seminal vesicle removal were still found to be sterile (0.0 ± 0.0; $P < 0.001$) (Fig. 1*E*); Moreover, copulatory plugs were not formed in female mice that were mated with male mice with seminal vesicles removed (Fig. 1*D*, *Bottom*), even though mating behavior, testosterone production, and spermatogenesis in these mice is normal (*SI Appendix*, Fig. S6). Both *SVS2*$^{-/-}$ mice and male mice that had undergone seminal vesicle removal showed failure of copulatory plug formation and leakage of the ejaculated sperm from the uterus, as evidenced by the presence of sperm in the vagina and decreased numbers of sperm in the uterus (Fig. 1*F*). The sperm number in the female reproductive tract was remarkably reduced because of a loss of plug formation. On the other hand, as described recently (13), loss of a copulatory plug strongly reduces the number of uterine sperm and lowers fertility but does not lead to severe subfertility or infertility. Therefore, it was unclear whether the infertility of *SVS2*$^{-/-}$ mice was due to the lack of sperm reaching the egg or other mechanisms.

To address this question, we developed a method for artificial insemination (AI) (Fig. 2*A* and *SI Appendix*, Fig. S7). Briefly, epididymal sperm (5×10^6 sperm/mL) with or without seminal vesicle secretions were injected directly into the uterus of female mice, followed by silicon, which filled the cervix and the vagina as a substitute for a copulatory plug, preventing the sperm from leaving the uterus. To assess sperm fertility in vivo, two-cell embryos developed in the oviduct were counted 25 h after sperm injection. Surprisingly, the direct injection of epididymal sperm into the uterus resulted in a significantly lower rate of two-cell embryo formation in the oviduct (20.4% ± 7.4%) compared with mice that had been injected with epididymal sperm and seminal vesicle secretions (76.0% ± 17.7%; $P = 0.019$) (Fig. 2*B*). To evaluate the effect of SVS2 as a decapacitation factor, we counted the number of acrosome-reacted sperm in the uterus 2 h after sperm injection. The rate of acrosomal reaction was dramatically increased when sperm were injected into the uterus without seminal vesicle secretions [82.7% ± 3.5% using FITC-labeled peanut agglutinin (PNA-FITC); 88.9% ± 1.4% using anti-IZUMO1 mAb; $P < 0.001$], compared with sperm injected with seminal vesicle secretions (PNA-FITC, 9.2% ± 3.1%; anti-IZUMO1, 12.9% ± 2.4%) or during normal copulation (PNA-FITC, 10.3% ± 2.8%; anti-IZUMO1, 14.1% ± 2.3%) (Fig. 2*C* and *SI Appendix*, Fig. S8*A*). These results suggest that the absence of seminal vesicle secretions strongly affects in vivo fertilization.

To assess the in vivo fertility of sperm ejaculated from *SVS2*$^{-/-}$ male mice, we introduced transgenes expressing GFP in the acrosome and RFP in the mitochondria [*B6D2F1-Tg (CAG/su9-DsRed2, Acr3-EGFP) RBGS002Osb*] (14) into the *SVS2*$^{-/-}$ background (*SVS2*$^{-/-}$*Tg*^{RBGS}) (*SI Appendix*, Fig. S8*B*). We then estimated the acrosome reaction rate for sperm ejaculated into female mice. We first confirmed that the disappearance of GFP fluorescence from sperm heads was consistent with the occurrence of an acrosome reaction detected by PNA-FITC and anti-IZUMO1 mAb, 3 h after sperm entered the uterus via copulation

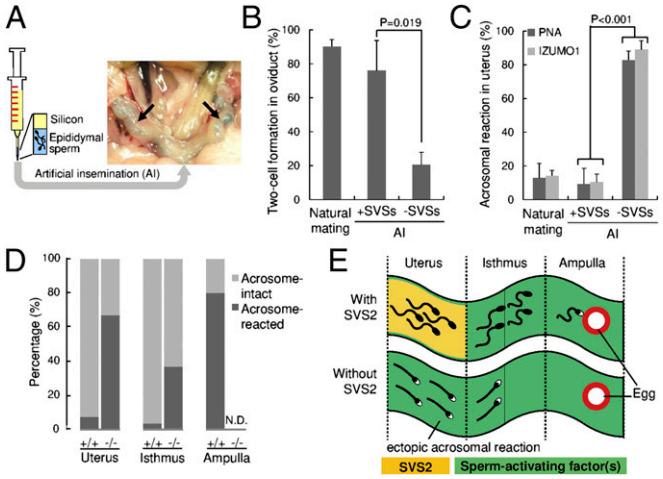

Fig. 2. Sperm fertility with or without SVS2 by AI using silicon as a substitute for the copulatory plug. (*A*) Experimental design of the AI procedure. Arrows, sperm solution coinjected with a blue dye in the uterine cavity. (*B*) Formation of two-cell embryos in oviducts by injection of sperm with or without SVSs using AI. Concomitantly, when female mice were mated with male mice, the number of two-cell embryos formed in oviducts was counted ($n = 6$). (*C*) Rates of acrosome-reacted sperm in the uterus by injection of sperm with or without SVSs using AI. Concomitantly, when female mice were mated with male mice, the number of acrosome-reacted sperm in the uterus was counted ($n = 3$). (*D*) Rates of acrosome-reacted sperm ejaculated from $SVS2^{-/-}$ mice or control mice ($SVS2^{+/+}$and $SVS2^{+/-}$) to the female reproductive tract ($n = 3$). In three parts of the reproductive tract, the number of acrosome-reacted sperm (RFP-positive and GFP-negative) was counted and compared with that of acrosome-intact sperm (RFP-positive and GFP-positive). (*E*) Schematic model of ectopic sperm activation in the absence of SVS2. Sperm with black heads, acrosome-intact sperm; sperm with white heads, acrosome-reacted sperm. Green substance, predicted sperm-activating factor(s).

(*SI Appendix*, Fig. S8*C*). When $SVS2^{-/-}Tg^{RBGS}$ male mice were mated with female mice, the ejaculated sperm were found to enter the uterus without plug formation, although the number of sperm inside the female reproductive tract was reduced compared with control $SVS2^{+/+}Tg^{RBGS}$ and $SVS2^{+/-}Tg^{RBGS}$ mice (*SI Appendix*, Figs. S9 and S10). Furthermore, in these two control mice nearly all sperm had intact acrosomes in the uterus and isthmus of the oviduct 3 h after sperm ejaculation (Fig. 2*D*). In the ampulla of oviduct, an acrosome reaction occurred in more than 80% of ejaculated sperm from the control mice (PNA-FITC, 83.3% ± 16.7%; anti-IZUMO1, 87.5% ± 12.5%) (Fig. 2*D*). In contrast, ejaculated sperm from $SVS2^{-/-}Tg^{RBGS}$ male mice had already undergone the acrosomal reaction inside the uterus (67.0% ± 2.4%) (Fig. 2*D*). In addition, ejaculated sperm from $SVS2^{-/-}Tg^{RBGS}$ male mice were rarely observed in the isthmus of the oviduct but were unable to move into the ampulla (Fig. 2*D*). Because the sperm of $SVS2^{-/-}Tg^{RBGS}$ male mice normally express two factors involved in sperm migration, namely ADAM3 and Catsper2 (*SI Appendix*, Fig. S11 *A* and *B*), we considered that the impaired migration to the oviduct was due to the absence of SVS2. We supposed that in the absence of SVS2 the ejaculated sperm would undergo an acrosomal reaction ectopically inside the uterus as a result of the sperm-activating factor(s) stored there, effectively blocking the entry of sperm into the oviduct (Fig. 2*E*).

To test this hypothesis, we next examined the sperm membrane collected from the uterus via electron microscopic analysis. The three groups examined were the epididymal sperm injected by AI with seminal vesicle secretions (+SVSs), with SVS2 (+SVS2), and without SVS2 (–SVS2). In the case of +SVSs or +SVS2, the sperm membrane remained intact in the uterus and became coated with the seminal vesicle secretions and SVS2 (Fig. 3 *A* and *B*). When the sperm were used for AI without SVS2, the cell and nuclear membranes were fractured not only in the acrosome but in all regions of the sperm (Fig. 3 *A* and *B*). To further examine the membrane disruption of the sperm in the uterus, the sperm were stained with propidium iodide (PI) and eosin (15). Consistent with the electron microscopic analysis, the rate of membrane-disrupted sperm was significantly higher without SVS2 (PI, 72.9% ± 3.4%, $P < 0.001$; eosin, 93.9% ± 2.3%, $P < 0.001$) than with SVS2 (PI, 12.8% ± 3.1%; eosin, 14.0% ± 4.7%) (Fig. 3*C*). From these results we concluded that intrauterine sperm died in the absence of SVS2.

To further examine this concept, we carried out immunohistochemical analysis of intrauterine sperm with or without SVS2 using anti-IZUMO1 mAb (Fig. 3 *D* and *E*). During sperm–egg fusion, IZUMO1 is translocated from the acrosomal membrane to the sperm plasma membrane at the time of acrosomal exocytosis (16), and its distribution is subsequently divided into two types, entire-head type (H-type) and equatorial segment type (17). We categorized the IZUMO1 distribution in the intrauterine sperm without SVS2 into an uncharacteristic type, namely the acrosomal-cap type (AC-type) (Fig. 3*D*). The rate of AC-type distribution was significantly higher in the sperm without SVS2 (83.7% ± 3.1%) than in the sperm mated naturally and the sperm with SVS2 (2.6% ± 0.8% and 0.9% ± 0.6%, respectively; $P < 0.001$) (Fig. 3*E*), indicating that the AC-type sperm were dead. To confirm the cytotoxic effect of uterine fluid (UF), sperm collected from the epididymides of $SVS2^{+/+}$ and $SVS2^{-/-}$ mice were incubated with UF. Consequently, sperm motility decreased in a time-dependent manner and was comparable between $SVS2^{+/+}$ and $SVS2^{-/-}$ mice (*SI Appendix*, Fig. S12 *A* and *B*); the rate of PI-positive dead sperm was similarly increased in both strains (*SI Appendix*, Fig. S12 *C* and *D*). On the other hand, the cytotoxic effect was absent in fluid collected from the ampulla of oviduct (*SI Appendix*, Fig. S13). In the sperm collected from $SVS2^{-/-}$ mice, CD46, whose deficiency in sperm accelerates spontaneous acrosomal reactions (18), was normally expressed and localized in the sperm head (*SI Appendix*, Fig. S11 *C* and *D*). Thus, our results suggest that intrauterine sperm die as a result of direct exposure to UF in the absence of SVS2.

Discussion

We previously reported that SVS2 acts as a decapacitation factor in IVF (10). As expected, the sperm ejaculated from $SVS2^{-/-}$ mice seemed to show ectopic activation in the uterine cavity, resulting in failure to reach the eggs in the oviduct (Figs. 1 and 2). However, further experiments revealed that the sperm are killed in the uterine cavity in the absence of SVS2 (Fig. 3). Thus, we concluded that the sperm transit through the spermicidal uterine environment from which SVS2 protects the sperm membrane (Fig. 4). In addition, the fertility of sperm that ascend beyond the uterus and the oviduct is strikingly higher than that of the epididymal sperm used for IVF (8), suggesting that sperm are selected in the female reproductive tract. Our finding opens the possibility that a competitive balance between death and survival in the uterus contributes to sperm selection.

In mammals, fertilization is the natural cell transplantation from males to females (19). When cell transplantation is performed for patients, such as those with acute leukemia, transplanted cells are exposed to the immune system of the hosts (20). The immune system in the female reproductive tract is believed to immunologically distinguish the sperm and fetus from pathogens (21). Our results suggest that ejaculated sperm may be treated as foreign objects in the uterus. Because fertilization occurs internally in animals such as mammals, birds, reptiles, and insects (22), the spermicidal system may be conserved in the female reproductive tract of other animals. In fact, in the polyandrous fly (*Scathophaga stercoraria*), sperm viability is significantly lower in

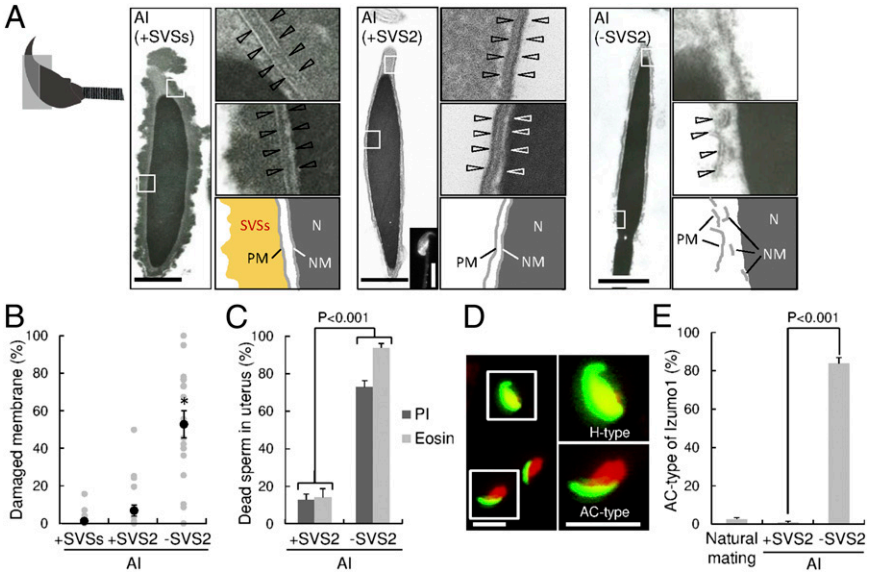

Fig. 3. SVS2-mediated protection of intrauterine sperm from membrane disruption. (*A*) Transmission electron microscopic (TEM) images. Diagram at far left indicates the orientation of sectioned heads of sperm. (*Left*) Sperm with SVSs; (*Center*) sperm with SVS2; (*Right*) sperm without SVS2. (*Left*, *Center*, and *Right*) Right upper and middle images are enlarged views of boxes in the left images, and diagrams are depicted in the right lower images. PM, plasma membrane; N, nucleus; NM, nuclear membrane. (Scale bars: 1 μm.) (*Center*, *Inset*) A fluorescent image of the sperm reacted with anti-SVS2 pAb. (Scale bar, 5 μm.) (*B*) Rates of broken membrane areas in TEM images ($n = 20$). *$P < 0.001$. (*C*) Rates of dead sperm in the uterus determined by staining with PI and eosin ($n = 3$). (*D*) Fluorescent images of sperm collected from the uterus by staining with anti-IZUMO1 mAb (green) and DAPI (red). (*Right*) Enlarged images of boxes at *Left*. H-type, fusion-capable sperm; AC-type, dead sperm. (Scale bars, 10 μm.) (*E*) Rate of sperm categorized as AC-type ($n = 3$).

the female sperm storage glands immediately after mating than in the male testis (23). If females have the intrinsic ability to kill sexually transmitted pathogens as well as sperm, then males would have had to develop a strategy against such a female spermicidal system. We consider that coevolution of these two systems may select highly specified sperm for fertility.

Cell death is induced in various ways that diverge morphologically and biochemically (24, 25). Cells exposed to natural inducers or cytotoxic substances undergo cell death involving a loss of membrane integrity, which is a hallmark of cell death (26). In animal sperm, the acrosome reaction is an exocytotic event in which membrane fusion takes place between the outer acrosomal membrane and the overlying plasma membrane to form transmembrane pores and allow release or exposure of their contents, resulting in membrane disruption (27). However, the membrane disruption induced by the acrosome reaction completely differs from the membrane disruption caused by cell death, because the integrity of the sperm plasma membrane is maintained throughout and after the acrosome reaction (28). Because the sperm plasma membrane was widely disrupted in the absence of SVS2 (Fig. 3), we concluded that the sperm was dead but not acrosome-reacted.

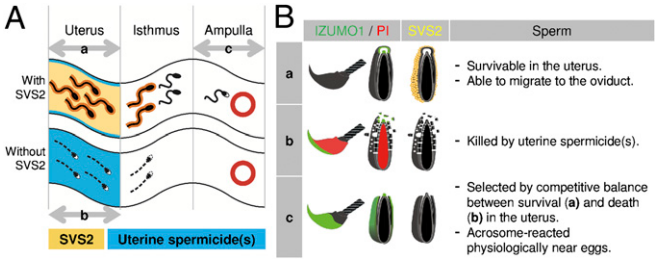

Fig. 4. Schematic model of the role of SVS2 in sperm protection in vivo. (*A*) Sperm migration in the female reproductive tract. Sperm with black heads, acrosome-intact sperm; sperm with white heads, acrosome-reacted sperm. Yellow, SVS2; blue, predicted maternal spermicide(s). a, acrosome-intact sperm penetrated the uterus after natural mating. b, membrane-disrupted dead sperm in the uterus in the absence of SVS2. c, acrosome-reacted sperm penetrated the ampulla. (*B*) Status of acrosomal and plasma membranes of sperm in the female reproductive tract. Categories a, b, and c correspond to those in *A*. Green, sperm membrane stained with anti-IZUMO1 mAb; red, sperm nucleus stained with PI.

In mammals, the seminal plasma is mainly secreted from seminal vesicles, the roles of which are discussed mainly with respect to plug formation (29), in addition to other aspects such as energy sources for sperm (30), regulation of sperm motility (31), and preparation of the uterine environment for implantation (21). In polyandrous mating systems, the seminal plasma plays a role in promoting the penetration of self-sperm and eliminating non-self-sperm. For example, the molecular evolution of *SEMG2*, one of the *SVS2* homologs, directly affects the biochemical dynamics of semen coagulation, suppressing fertilization success by copulation with rival males in primates (32). Furthermore, the phenomenon of sperm survival with the aid of the seminal plasma is often found in the animal kingdom, for example in pigs (33) and honey bees (34). Our results provide direct evidence for a molecular mechanism underlying sperm survival whereby the seminal plasma in the uterus protects the sperm. This proposes the concept of "competitive sperm selection" between males and females.

Currently, in cases of male infertility, doctors and patients are often left with few options other than IVF and/or intracytoplasmic sperm injection, mainly owing to the lack of knowledge of in vivo fertilization (35). A recent study revealed that seminal vesicle composition has multiple functions in the female reproductive tract, which not only affect sperm protection and selection before fertilization but also indirectly affect the development and metabolism of progeny (9). The knowledge gained in this and our studies may contribute to the clinical diagnosis of infertility and improve the probability of reproduction. Moreover, taking the functions of SVS2 in the uterus into consideration may lead to the improvement of AI birth rates.

Materials and Methods

Antibodies and Chemicals. The mAbs against IZUMO1 and anti-CD46, kindly provided by M. Okabe (Osaka University, Osaka), were used for immunostaining and immunoblotting (18, 36). For immunoblotting, a polyclonal antibody (pAb) was produced in rabbits by immunization with an SVS2 peptide with the following sequence: RKNFNPGNYFTKGGADC (No. SVS2-2). Mouse anti-ADAM3 mAb was purchased from Upstate Biotechnology, and anti-Catsper2 pAb was purchased from Aviva System Biology. Alexa 488-conjugated IgG (Molecular Probes) was used as a secondary antibody. Horseradish peroxidase-conjugated secondary antibodies (Sigma-Aldrich) were used for immunoblotting. Nuclei were counterstained with DAPI (Wako Pure Chemical Industries).

Generation of *SVS2*$^{-/-}$ Mice. Two types of targeting vectors were designed to remove (*i*) whole exons and (*ii*) the portion of the *SVS2* gene spanning exons 1–2 (*SI Appendix*, Fig. S1 *A* and *B*) and were conventionally electroporated into 129/Sv strain-derived ES cells after linearization. Recombinant ES clones were identified by PCR and Southern blot analyses (*SI Appendix*, Fig. S1 *C–F*). Two recombinant ES cell lines (formed by electroporation of each of two kinds of targeting vectors) were microinjected into C57BL/6N strain-derived blastocysts, and the male chimeric mice were obtained. Subsequently, these mice were crossed with C57BL/6N female mice to yield heterozygote offspring. Next, to produce homozygotes, male and female heterozygotes were intercrossed and backcrossed to the C57BL/6N background.

All mice were housed under specific pathogen-free controlled conditions. Food and water were available ad libitum. All animal experiments were performed according to protocols approved by the Institutional Animal Care and Use Committee at the National Institute for Child Health and Development.

Surgical Removal of Accessory Sex Organs. Eight-week-old male ICR mice were anesthetized [2.5% (wt/vol) tribromoethanol, 10 μL/g body weight, intraperitoneally], and depending on the case, either coagulating glands or seminal vesicles were surgically removed via a midventral incision (Fig. 1*D*).

Analysis of Sperm Migration. The sperm location in the female reproductive tract was determined histochemically by hematoxylin and eosin staining. At 3 h after copulation, the female reproductive tract containing the ejaculated sperm was fixed and prepared for paraffin sectioning (thickness, 6 μm). In four parts of the female reproductive tract (vagina, uterus, isthmus, and ampulla of oviduct), the number of sperm head detected at the lumen of each tissue was counted in five consecutive slices. No sperm in the tissue were confirmed by all consecutive slices. Because the oviduct at 3 h after copulation contained ejaculated sperm at greater levels than that at 2 h, we observed the female reproductive tract at 3 h after sperm insemination.

Artificial Insemination. To study the involvement of seminal vesicle secretions in fertilization, sperm were isolated from the epididymides of 8-wk-old male C57BL/6N mice and directly injected into the uterus of 8-wk-old female C57BL/6N mice with a syringe. Before sperm collection the female mice were determined to be in the estrus phase using vaginal smear cytology (37). As depicted in Fig. 2*A* and *SI Appendix*, Fig. S7, a 50-μL aliquot of the epididymal sperm suspension (5×10^7 sperm/mL) was prepared in a yellow tip attached to a 1-mL syringe containing silicon and then injected from the cervix into the uterus with or without the vesicle secretions. The seminal vesicle secretions were surgically collected from one male mouse and dissolved in 1 mL of modified Krebs–Ringer bicarbonate solution (TYH medium), and then centrifuged for 5 min at 10,000 × *g* at room temperature. The supernatant containing soluble proteins from the seminal vesicle was used as SVS and mixed with approximately one-tenth of the volume of the sperm suspension. Silicon was used as a substitute for a copulating plug. Female reproductive tracts from the vagina to oviduct were excised 3 h after sperm injection to allow for sperm migration and for the acrosomal status to be immunocytologically examined. In addition, two-cell embryos and unfertilized eggs were recovered from the oviducts by flushing with TYH medium 24 h after the sperm injection. The numbers of two-cell embryos and unfertilized eggs were counted and used for estimating the success rate of fertilization.

Immunoblotting. The internal fluids were collected from seminal vesicles of male mice and then subjected to Coomassie Brilliant Blue (CBB) staining and immunoblotting as previously described (10). Briefly, the seminal vesicle fluid from one male mouse was diluted in 1 mL of PBS and then solubilized in an equal volume of 2× Laemmli SDS sample buffer. The solubilized samples were resolved by SDS/PAGE on 10% (wt/vol) acrylamide gels and then transferred to Immobilon-FC (Millipore). Mouse seminal vesicle secretion has been reported to consist of up to seven clearly identifiable components, SVS I–VII (38, 39). The detection of immune complexes formed by the proteins of interest and primary antibodies was performed by enzyme-linked color development with horseradish peroxidase conjugated to secondary antibodies. The sperm were collected from the epididymides and also subjected to immunoblotting as described above.

Electron Microscopic Analysis. The sperm were collected from the uterus after AI and then fixed with glutaraldehyde and osmic acid solutions. Ultra-thin sections were prepared as previously described (40). To further quantify the membrane integrity, we measured the length of the damaged membrane per total length of the sperm plasma membrane using Adobe Illustrator CS5 software.

Histochemical Analysis. The male mice were killed, and their testes were examined histochemically by hematoxylin and eosin staining, as described previously (41).

Estimation of Male Fertility in Vivo and in Vitro. To evaluate male fertility in vivo, numbers of pups delivered from 8- to 12-wk-old female mice were recorded after a 2-wk mating period, during which female mice were housed with 8- to 12-wk-old male mice.

For IVF, eggs were collected from superovulated C57BL/6N female mice (8–12 wk old) 14–16 h after human chorionic gonadotropin (hCG) injection (42). The sperm collected from the epididymides of 8- to 12-wk-old male mice were capacitated by incubating in TYH medium for 120 min before insemination. The final concentration of the sperm added to the eggs was 1.5×10^5 sperm/mL.

Detection of Acrosome-Reacted Sperm in the Female Reproductive Tract. To evaluate the acrosomal status of sperm in female reproductive tracts, anti-IZUMO1 mAb and PNA-FITC (Sigma) were used. For immunostaining, sperm were collected from the uterus and fixed for 20 min at 4 °C in a solution containing 4% (wt/vol) paraformaldehyde and 0.1% polyvinylpyrrolidone. After being washed in PBS, sperm were immunostained with anti-IZUMO1 mAb for 1 h at 4 °C and then washed three times in TYH medium, according to previously described methods (42). To further monitor acrosomal status, sperm were collected from the uterus and smeared onto glass slides. Sperm were then air-dried, permeabilized, and fixed with 100% methanol for 10 min at room temperature. After being washed in PBS, sperm were incubated with PNA-FITC in PBS for 10 min at 37 °C and washed three times for 5 min in PBS (10). The fluorescent images were captured by a laser scanning confocal microscope (LSM 510 model; Carl Zeiss Microimaging Inc.). Acrosome-reacted sperm were reacted with anti-IZUMO1 mAb and unreacted with PNA-FITC (10).

To detect acrosome-reacted sperm inside the female reproductive tract, we used transgenic sperm expressing GFP in their acrosomes and RFP in their mitochondria [*B6D2F1-Tg (CAG/su9-DsRed2, Acr3-EGFP) RBGS002Osb*] (14). When the transgenes were introduced into the *SVS2*$^{-/-}$ background, the epididymal acrosome-intact sperm produced in *SVS2*$^{-/-}$ mice could be visualized using dual fluorescence. At 3 h after copulation, the female reproductive tracts containing the ejaculated sperm were fixed and prepared for frozen sections (thickness, 20 μm). In three parts of the female reproductive tract (uterus, isthmus, and ampulla of oviduct), the number of acrosome-reacted sperm (RFP-positive and GFP-negative) was counted and compared with that of acrosome-intact sperm (RFP-positive and GFP-positive).

Measurement of Sperm Motility. For measurement of sperm motility and hyperactivation, CASA operated by IVOS software (Hamilton-Thorne Biosciences) was used, as previously described (42). An aliquot of the capacitated sperm suspension was transferred into a prewarmed counting chamber (depth, 100 mm), and >200 sperm were examined for each sample using standard settings (30 frames acquired at a frame rate of 60 Hz at 37 °C), as previously described. The motility of hyperactivated sperm was determined by using the SORT function of the IVOS software. Sperm were classified as hyperactivated when the trajectory met the following criteria: curvilinear velocity ≥180 μm/s, linearity ≤38%, and amplitude of lateral head displacement ≥9.5 μm.

Generation of BAC Transgenic Mice and Rescue Experiment. A BAC clone (RP23-377B11) containing the full-length mouse *SVS2* gene was purchased from BACPAC Resources Center (Invitrogen) and microinjected into eggs (43). For

the rescue experiment, transgenic mouse lines expressing SVS2 under the control of an *SVS2* native promoter were produced and transferred onto the *SVS2*$^{-/-}$ background.

Detection of the Spermicidal Effect of UF. To evaluate the percentage of dead sperm influenced by UF, the epididymal sperm without SVS2 were incubated in TYH medium containing 10% (vol/vol) UF and oviductal fluid for 3 h and then stained with both 10 μg/mL PI (Sigma) and 10 μg/mL Hoechst 33342 (Invitrogen). After estrus phase was determined by vaginal smear cytology (37), the UF was collected from each of the uterine horns of 8- to 10-wk-old C57BL/6N female mice using a micropipette. The oviductal fluid was collected from the ampulla of oviduct in superovulated C57BL/6N female mice 14–16 h after hCG injection. For each sample, after >200 sperm were examined, doubly PI- and Hoechst 33342-positive sperm were counted as dead sperm, whereas only Hoechst 33342-positive sperm were counted as living sperm.

Statistical Analysis. Comparisons were made using one-way analysis of variance following Scheffé's method, the Mann-Whitney *U* test, or Fisher's exact test. Statistical significance was defined as $P < 0.05$. Results are expressed as the mean ± SEM.

ACKNOWLEDGMENTS. We thank M. Okabe for providing the anti-IZUMO1 mAb, as well as M. Morisawa, T. Iwamoto, and N. Inoue for critical discussions. This work was supported by a grant from the Ministry of Health, Labor and Welfare, and a grant-in-aid for scientific research from the Ministry of Education, Culture, Sports, and Technology of Japan.

1. Suarez SS (2006) in *Knobil and Neill's Physiology of Reproduction*, ed Neill JD (Academic, New York), 3rd Ed, pp 113–145.
2. Chang MC (1957) A detrimental effect of seminal plasma on the fertilizing capacity of sperm. *Nature* 179(4553):258–259.
3. Bedford JM, Chang MC (1962) Removal of decapacitation factor from seminal plasma by high-speed centrifugation. *Am J Physiol* 202(1):179–181.
4. Fraser LR (1984) Mouse sperm capacitation in vitro involves loss of a surface-associated inhibitory component. *J Reprod Fertil* 72(2):373–384.
5. Nixon B, et al. (2006) The identification of mouse sperm-surface-associated proteins and characterization of their ability to act as decapacitation factors. *Biol Reprod* 74(2): 275–287.
6. Lu CH, et al. (2011) SERPINE2, a serine protease inhibitor extensively expressed in adult male mouse reproductive tissues, may serve as a murine sperm decapacitation factor. *Biol Reprod* 84(3):514–525.
7. Fukami K, et al. (2001) Requirement of phospholipase Cdelta4 for the zona pellucida-induced acrosome reaction. *Science* 292(5518):920–923.
8. Suarez SS, Pacey AA (2006) Sperm transport in the female reproductive tract. *Hum Reprod Update* 12(1):23–37.
9. Bromfield JJ, et al. (2014) Maternal tract factors contribute to paternal seminal fluid impact on metabolic phenotype in offspring. *Proc Natl Acad Sci USA* 111(6): 2200–2205.
10. Kawano N, Yoshida M (2007) Semen-coagulating protein, SVS2, in mouse seminal plasma controls sperm fertility. *Biol Reprod* 76(3):353–361.
11. Kawano N, Yoshida K, Iwamoto T, Yoshida M (2008) Ganglioside GM1 mediates decapacitation effects of SVS2 on murine spermatozoa. *Biol Reprod* 79(6):1153–1159.
12. Olson EN, Arnold HH, Rigby PW, Wold BJ (1996) Know your neighbors: Three phenotypes in null mutants of the myogenic bHLH gene MRF4. *Cell* 85(1):1–4.
13. Dean MD (2013) Genetic disruption of the copulatory plug in mice leads to severely reduced fertility. *PLoS Genet* 9(1):e1003185.
14. Hasuwa H, et al. (2010) Transgenic mouse sperm that have green acrosome and red mitochondria allow visualization of sperm and their acrosome reaction in vivo. *Exp Anim* 59(1):105–107.
15. Graham JK, Kunze E, Hammerstedt RH (1990) Analysis of sperm cell viability, acrosomal integrity, and mitochondrial function using flow cytometry. *Biol Reprod* 43(1): 55–64.
16. Emoto K, et al. (1996) Redistribution of phosphatidylethanolamine at the cleavage furrow of dividing cells during cytokinesis. *Proc Natl Acad Sci USA* 93(23): 12867–12872.
17. Satouh Y, Inoue N, Ikawa M, Okabe M (2012) Visualization of the moment of mouse sperm-egg fusion and dynamic localization of IZUMO1. *J Cell Sci* 125(Pt 21): 4985–4990.
18. Inoue N, et al. (2003) Disruption of mouse CD46 causes an accelerated spontaneous acrosome reaction in sperm. *Mol Cell Biol* 23(7):2614–2622.
19. Ikawa M, Inoue N, Benham AM, Okabe M (2010) Fertilization: A sperm's journey to and interaction with the oocyte. *J Clin Invest* 120(4):984–994.
20. Thomas ED, et al. (1977) One hundred patients with acute leukemia treated by chemotherapy, total body irradiation, and allogeneic marrow transplantation. *Blood* 49(4):511–533.
21. Schuberth HJ, et al. (2008) Immunological responses to semen in the female genital tract. *Theriogenology* 70(8):1174–1181.
22. Snook RR, Hosken DJ, Karr TL (2011) The biology and evolution of polyspermy: insights from cellular and functional studies of sperm and centrosomal behavior in the fertilized egg. *Reproduction* 142(6):779–792.
23. Bernasconi G, Hellriegel B, Heyland A, Ward PI (2002) Sperm survival in the female reproductive tract in the fly *Scathophaga stercoraria* (L.). *J Insect Physiol* 48(2): 197–203.
24. Elmore S (2007) Apoptosis: A review of programmed cell death. *Toxicol Pathol* 35(4): 495–516.
25. Orrenius S, Nicotera P, Zhivotovsky B (2011) Cell death mechanisms and their implications in toxicology. *Toxicol Sci* 119(1):3–19.
26. McNeil PL, Steinhardt RA (1997) Loss, restoration, and maintenance of plasma membrane integrity. *J Cell Biol* 137(1):1–4.
27. Toshimori K (2009) Dynamics of the mammalian sperm head: Modifications and maturation events from spermatogenesis to egg activation. *Adv Anat Embryol Cell Biol* 204:5–94.
28. Uto N, Yoshimatsu N, Lopata A, Yanagimachi R (1988) Zona-induced acrosome reaction of hamster spermatozoa. *J Exp Zool* 248(1):113–120.
29. Mann T, Lutwak-Mann C (1981) *Male Reproductive Function and Semen* (Springer, Berlin).
30. Mann T, Lutwak-Mann C (1948) Studies on the metabolism of semen. 4. Aerobic and anaerobic utilization of fructose by spermatozoa and seminal vesicles. *Biochem J* 43(2):266–270.
31. Luo CW, Lin HJ, Chen YH (2001) A novel heat-labile phospholipid-binding protein, SVS VII, in mouse seminal vesicle as a sperm motility enhancer. *J Biol Chem* 276(10): 6913–6921.
32. Dorus S, Evans PD, Wyckoff GJ, Choi SS, Lahn BT (2004) Rate of molecular evolution of the seminal protein gene SEMG2 correlates with levels of female promiscuity. *Nat Genet* 36(12):1326–1329.
33. Rozeboom KJ, Troedsson MH, Hodson HH, Shurson GC, Crabo BG (2000) The importance of seminal plasma on the fertility of subsequent artificial inseminations in swine. *J Anim Sci* 78(2):443–448.
34. King M, Eubel H, Millar AH, Baer B (2011) Proteins within the seminal fluid are crucial to keep sperm viable in the honeybee *Apis mellifera*. *J Insect Physiol* 57(3):409–414.
35. Hansen M, Bower C, Milne E, de Klerk N, Kurinczuk JJ (2005) Assisted reproductive technologies and the risk of birth defects—a systematic review. *Hum Reprod* 20(2): 328–338.
36. Inoue N, Ikawa M, Isotani A, Okabe M (2005) The immunoglobulin superfamily protein Izumo is required for sperm to fuse with eggs. *Nature* 434(7030):234–238.
37. Gurtovenko AA, Vattulainen I (2007) Lipid transmembrane asymmetry and intrinsic membrane potential: Two sides of the same coin. *J Am Chem Soc* 129(17):5358–5359.
38. Chen YH, Pentecost BT, McLachlan JA, Teng CT (1987) The androgen-dependent mouse seminal vesicle secretory protein IV: Characterization and complementary deoxyribonucleic acid cloning. *Mol Endocrinol* 1(10):707–716.
39. Fawell SE, McDonald CJ, Higgins SJ (1987) Comparison of seminal vesicle secretory proteins of rodents using antibody and nucleotide probes. *Mol Cell Endocrinol* 50(1-2):107–114.
40. Iuchi Y, et al. (2009) Peroxiredoxin 4 knockout results in elevated spermatogenic cell death via oxidative stress. *Biochem J* 419(1):149–158.
41. Papaioannou MD, et al. (2009) Sertoli cell Dicer is essential for spermatogenesis in mice. *Dev Biol* 326(1):250–259.
42. Kawano N, et al. (2010) Mice lacking two sperm serine proteases, ACR and PRSS21, are subfertile, but the mutant sperm are infertile in vitro. *Biol Reprod* 83(3):359–369.
43. Antoch MP, et al. (1997) Functional identification of the mouse circadian Clock gene by transgenic BAC rescue. *Cell* 89(4):655–667.